



# Preparation, characterization and mechanical properties of continuous mullite fibers derived from the diphasic sol-gel route

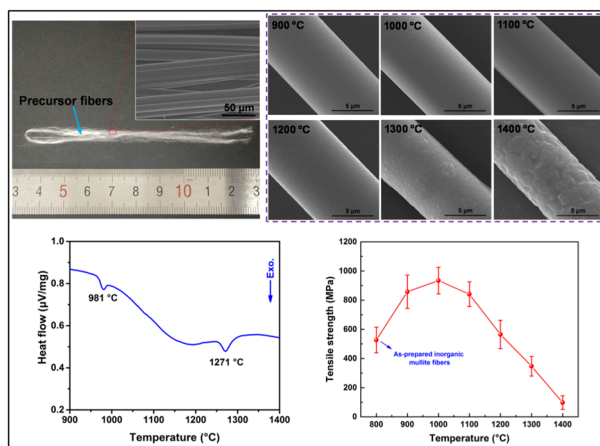
Yangrui Gao<sup>1</sup> · Wensheng Liu<sup>1</sup> · Xiaolei Song<sup>1</sup> · Qiang Liu<sup>1</sup> · Shuwei Yao<sup>1</sup> · Juan Wang<sup>1</sup> · Qingshan Cai<sup>1</sup> · Yunzhu Ma<sup>1</sup>

Received: 12 May 2019 / Accepted: 10 July 2019 / Published online: 20 July 2019  
© Springer Science+Business Media, LLC, part of Springer Nature 2019

## Abstract

In the present work, continuous mullite fibers were fabricated through the diphasic sol-gel route using aluminum isopropoxide (AIP) and aluminum nitrate (AN) as the alumina sources and colloidal silica as the silica source. Fiber processing was achieved via draw-spinning method. Amorphous inorganic mullite fibers with smooth and dense features, as well as designed chemical composition and uniform elemental distribution, were obtained by pyrolysis of the continuous precursor fibers at the ending temperature of 800 °C in air. The microstructure and mechanical properties of the samples sintered at elevated temperatures were investigated. Differential thermal analysis (DTA) showed two exothermic peaks at 978 and 1271 °C assigned to the crystallization of  $\gamma$ -Al<sub>2</sub>O<sub>3</sub> and mullite phase, respectively. X-ray powder diffraction (XRD) results verified the typical phase transformation route of diphasic mullite while sintering. Transmission electron microscopy (TEM) and scanning electron microscopy (SEM) showed a rapid grain growth after the mullite phase had formed. As the sintering temperatures increased, the filament tensile strength of the mullite fibers first increased and then decreased, reaching a maximum value of 934 MPa at 1000 °C.

## Graphical Abstract



✉ Juan Wang  
wangjuan@csu.edu.cn  
✉ Qingshan Cai  
caiqingshan@csu.edu.cn  
✉ Yunzhu Ma  
zhuzipm@csu.edu.cn

<sup>1</sup> National Key Laboratory of Science and Technology for National Defence on High-strength Structural Materials, Central South University, 410083 Changsha, China

## Highlights

- Continuous and homogeneous mullite fibers were prepared through the diphasic sol-gel route.
- Alumina sol fabricated by AIP and AN was used to prepare diphasic mullite sol for the first time.
- Smooth and dense surface remained at 900–1100 °C due to the small  $\gamma$ -Al<sub>2</sub>O<sub>3</sub> grains.
- Rapid grain growth occurred after 1200 °C was ascribed to the formation of mullite phase.
- A maximum tensile strength of 934 MPa was acquired after sintering the fibers at 1000 °C.

**Keywords** Mullite fibers · Diphasic sol · Microstructure · Mechanical properties · Draw-spinning

## 1 Introduction

Continuous mullite (3Al<sub>2</sub>O<sub>3</sub>·2SiO<sub>2</sub>) fibers are important ceramic materials for their wide applications in areas such as insulation, filtration, catalyst, etc. or as reinforcements for ceramic matrix composites (CMCs) [1–4]. They have drawn a lot of attention due to their low thermal conductivity, outstanding dielectric properties and excellent chemical stability [5, 6]. Considering the actual use of such material at high temperatures in air, development of the fibers with good thermal stability is becoming increasingly important.

The sol-gel method is one of the most commonly used approaches to fabricate mullite fibers due to its capacity for producing ceramics with high purity and homogeneity [7, 8]. It is well known that mullite precursor sol can be divided into monophasic sol and diphasic sol according to the homogeneity degree of aluminum and silicon [9]. In recent years, many researchers have fabricated mullite fibers successfully through the monophasic sol-gel route in the laboratory [10, 11]. However, nearly all the commercial mullite fibers are derived from the diphasic sol-gel route [12–14]. This is because that the mullite formation temperatures of the diphasic products (>1200 °C) are much higher than that of the monophasic products (<1000 °C) [9]. In this case, the diphasic-gels-derived mullite fibers are more stable in structure and properties while applied in high-temperature conditions.

To prepare the diphasic mullite sol, a homogeneous and stable alumina sol is acquired. As reported by literature [15, 16], the alumina sol used to produce commercial mullite fibers was synthesized using aluminum powder as the source. The aluminum powders are added into the mixture of water, formic acid, and acetic acid, and are stirred at a set temperature. However, a large amount of hydrogen gas generates during the dissolving process. Such inflammable gas will increase the risk in the actual production process. Besides, the reactions are exothermic when the aluminum powders are dissolving, which make the defined reaction temperature and the sol properties difficult to control. Thus, it is interesting to further examine the fabrication of mullite fibers using alumina sol from a simple, safe and controllable way. Aluminum isopropoxide (AIP), often used coupled with aluminum nitrate (AN), has

been proved to be a suitable alumina precursor [17, 18]. No inflammable gas formed and the reaction degree is easy to control during the sol preparation process, revealing a promising application prospect of the precursor.

On the basis of the above introduction, in the present study, continuous mullite fibers derived from the diphasic sol-gel route were fabricated via draw-spinning method [19]. Alumina sol was prepared using AIP and AN as the sources. Commercial colloidal silica was used as the silica source. Continuous, smooth and dense precursor mullite fibers were pyrolytic treated in the air at the ending temperature of 800 °C first. Then the fibers were sintered at elevated temperatures, and the microstructure and room temperature mechanical properties were studied in detail.

## 2 Experimental

### 2.1 Raw materials

AIP (C<sub>9</sub>H<sub>21</sub>AlO<sub>3</sub>) and AN (Al(NO<sub>3</sub>)<sub>3</sub>·9H<sub>2</sub>O) purchased from Aladdin Chemistry Co. Ltd. was used as the alumina sources. Commercial colloidal silica (LUDOX<sup>®</sup> LS) with a SiO<sub>2</sub> content of 30 wt. % and an original pH value of 8.2 obtained from Sigma-Aldrich (St Louis, USA) was used as the silica source. Nitric acid (HNO<sub>3</sub>) bought from Sino-pharm Chemical Reagent Co., Ltd. was used to adjust the pH value of colloidal silica. All of these reagents were used without further purification. Deionized water prepared in the laboratory was used as the solvent.

### 2.2 Sample preparation

A total of 30 g AN was dissolved into 115.2 ml deionized water at room temperature first, then 40.8 g AIP was added and stirred for 12 h. After refluxing at 80 °C for 10 h, a transparent and homogeneous alumina sol was obtained. For the commercial colloidal silica, dilute HNO<sub>3</sub> (3 wt. %) was added to adjust the pH from 8.2 to 2.3. Zeta-potential analysis showed that the colloid particles in the pre-prepared alumina sol and acidulated colloidal silica all charged positive charge. In this case, no precipitation generated when mixing the two sols. The mass percentages of

**Fig. 1** **a** Optical photograph and **b** SEM images of mullite precursor fibers

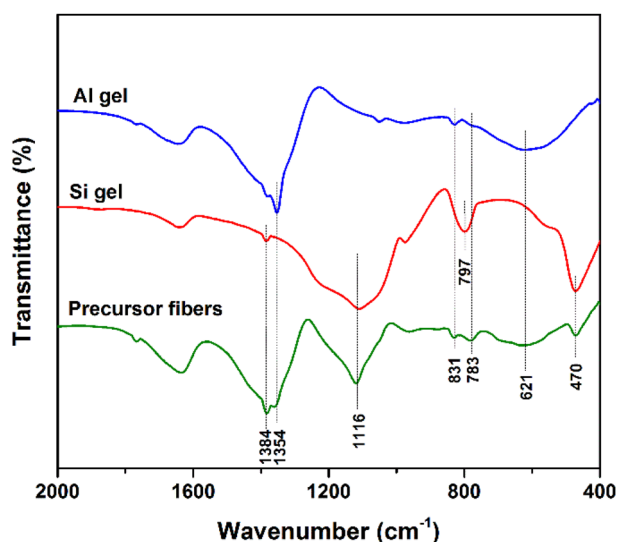
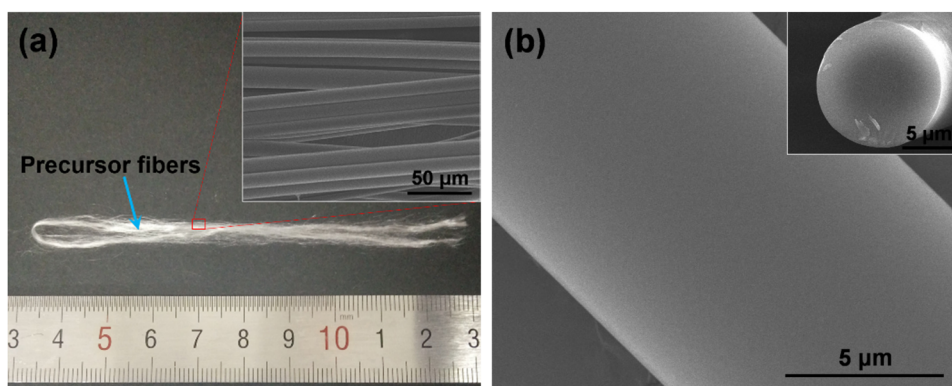


**Fig. 2** FT-IR spectra of **a** alumina gel, **b** silica gel and **c** precursor gel fibers in the 2000–400  $\text{cm}^{-1}$  range

$\text{Al}_2\text{O}_3$  and  $\text{SiO}_2$  for the mullite fibers were designed to be 68 and 32 wt. %, respectively. The transparent mullite precursor sol was concentrated using a rotary evaporator (RE6000 A, Yarong, China) to acquire the spinning dope with a suitable viscosity. Continuous precursor fibers were prepared via drawn-spinning method and collected by a rotating roller. The resulting fibers were dried at 60 °C for 12 h to remove the residual solvent for further treatment. The pyrolysis process was conducted using a muffle furnace by heating the fibers to 800 °C at a heating rate of 2 °C/min in air and maintaining at the ending temperature for 1 h. Then the amorphous inorganic mullite fibers were sintered at 900 to 1400 °C for 0.5 h to study the microstructure and mechanical properties at elevated temperatures.

### 2.3 Characterization method

Fiber morphology was examined by scanning electron microscopy (SEM, Nova Nano230, FEI, USA).

Thermogravimetry-differential thermal analysis (TG-DTA) analysis of precursor nanofibers was performed on a thermoanalyzer (STA-449F3, Netzsch, German) at a heating rate of 20 °C/min in an air atmosphere. X-ray powder diffraction (XRD) data of mullite nanofibers were recorded by a diffractometer (D8 Advance, Bruker, German) using  $\text{CuK}\alpha$  radiation in the region of  $10 < 2\theta < 80^\circ$ . Crystal grains in the mullite fibers were observed using transmission electron microscopy (TEM, JEM-2100F, JEOL, Japan). Filament tensile strength was measured by a fiber strength tester (XS(08)XT-3, XuSai, China) using a gauge length of 15  $\mu\text{m}$  and a traveling speed of 1 mm/min at room temperature. The fiber cross-sectional area was acquired by SEM measurement. Thirty fibers for each sample were tested to acquire the average strength values.

## 3 Results and discussion

### 3.1 Morphology and chemical structure of precursor fibers

Figure 1 displays the optical photograph and SEM images of mullite precursor fibers. As revealed in Fig. 1a, continuous precursor fibers with lengths of several tens of centimeters, uniform diameters, straight and cylindrical structure were obtained. The fiber diameters were in the range of 8–13  $\mu\text{m}$ . Figure 1b showed that the fiber surface was smooth and the fiber inner was dense, indicating that no defects like voids or cracks generated during the preparation process. All these results revealed that the spinning dope was suitable to be processed into fiber products.

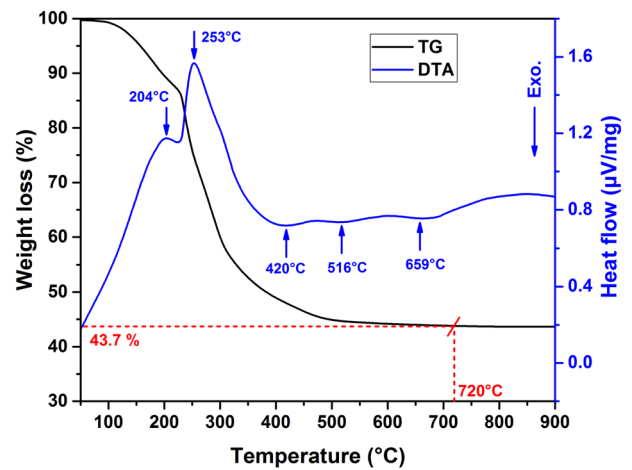
Figure 2 shows the FT-IR spectra of alumina gel, silica gel and precursor gel fibers in the 2000–400  $\text{cm}^{-1}$  range and Table 1 lists the corresponding band locations and assignments derived from the FT-IR spectra. For the gel fibers, the peak at around 1636  $\text{cm}^{-1}$  was ascribed to the presence of  $\text{H}_2\text{O}$ . The band at 1384  $\text{cm}^{-1}$  was due to the  $\text{N}=\text{O}$  symmetric stretching vibration in  $\text{NO}_3^-$  from the alumina and silica gel [11, 20]. The peaks at 1217, 1116,

557 and 470  $\text{cm}^{-1}$  were corresponded to the Si–O–Si groups in  $\text{SiO}_2$  [11, 20]. The peaks located in 1046 and 780  $\text{cm}^{-1}$  were assigned to the Al–OH bend [20, 21], while the bands observed at 693, 621 and 470  $\text{cm}^{-1}$  were attributed to the Al–O stretch in  $\text{AlO}_6$  normally [21–23]. In addition, the

band at 413  $\text{cm}^{-1}$  was caused by the bending vibration of Al–O–Al [21]. From these results, it could be concluded that the majority characteristic peaks of alumina gel and silica gel retained in the gel fibers and no other new peak emerged during the mixing process. This was evidence showing that the synthesized mullite precursor gel fibers belonged to the diphasic gel fibers [24].

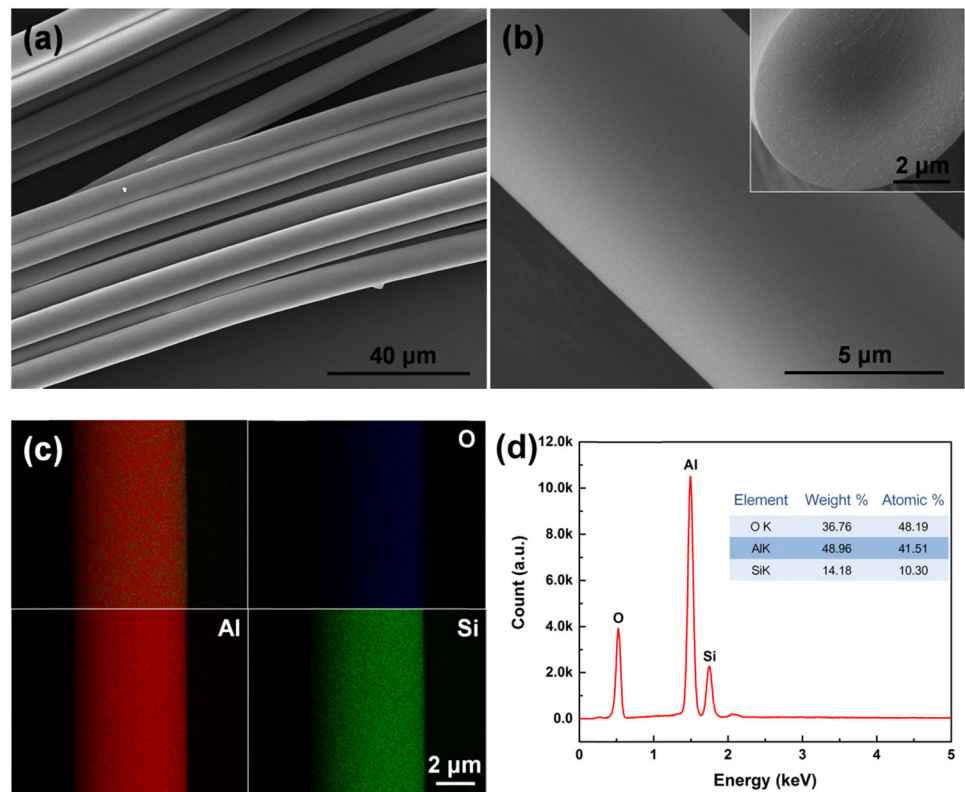
**Table 1** Band locations and assignments derived from FT-IR spectra of alumina gel, silica gel and precursor gel fibers

Al gel	Si gel	Precursor fibers	Assignment [11, 20–23]
1639	1637	1636	$\text{H}_2\text{O}$
1382	1385	1384	Ionic $\text{NO}_3^-$ stretch
1354	—	1354	C–H bend
—	1221	1217	Asym Si–O–Si stretch
—	1117	1116	Asym Si–O–Si stretch
1050	—	1046	Al–OH bend
—	973	969	Si–O–Si stretch
830	—	831	Al–O stretch in $\text{AlO}_4$
—	797	—	Si–OH
778	—	780	Al–OH bend
692	—	693	Al–O stretch in $\text{AlO}_6$
621	—	621	Al–O stretch in $\text{AlO}_6$
—	560	557	O–Si–O stretch
—	469	470	Al–O stretch in $\text{AlO}_6$ , O–Si–O bend
411	—	413	Al–O–Al bend



**Fig. 3** TG-DTA curves of the precursor fibers in the 50–900 °C temperature range

**Fig. 4** a, b SEM images, c elemental mappings and d EDS spectrum of the pyrolytic mullite fibers



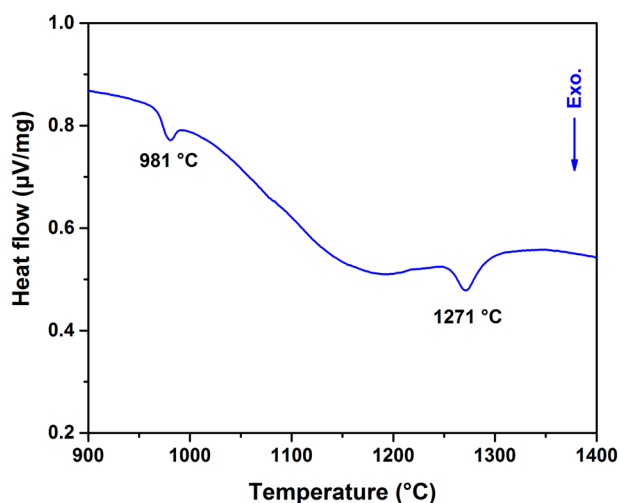


Fig. 5 DTA curve of the precursor fibers in the 900–1400 °C temperature range

### 3.2 Morphology and composition of pyrolytic mullite fibers

TG-DTA curves of the mullite precursor fibers are shown in Fig. 3. As evident from the TG curve, three major mass losses occurred when heating the fibers in the air. A mass loss of ~ 13.2 wt. % below 224 °C induced by the removal of free and crystal water was found. It was associated with the endothermic peak emerged at 204 °C in the DTA curve. As heating temperatures increased to 310 °C, the second mass loss of ~ 23.3 wt. % was observed. This was caused by the decomposition of nitrate and organic groups, which was corresponded to an endothermic peak located at 253 °C in the DTA curve. While from 310 to 720 °C, the third mass loss of ~ 13.6 wt. % caused by the decomposition of residual organics and the removal of decomposed products was detected. Such a conclusion was confirmed by the three broad exothermic peaks at 420, 516 and 659 °C in the DTA curve. No obvious mass loss was found at temperatures higher than 720 °C, revealing that the organics in the fibers had decomposed completely and the decomposed products had been removed entirely. In addition, no exothermic peak assigned to the onset of crystallization was found below 900 °C. Since the pyrolytic temperature was only 800 °C, the amorphous state for the fiber product was predicted.

Figure 4 shows the SEM images, elemental mappings and EDS spectrum of the pyrolytic mullite fibers. As evident from Fig. 4a, b, after the pyrolytic treatment, continuous, smooth and dense features of the fibers retained and no obvious voids or cracks were observed in the fiber inner. The fiber diameters range was measured to be 6–10 μm, which was smaller than that of the precursor fibers. This was due to the decomposition of the organics in the precursor. The elemental mappings presented in Fig. 4c

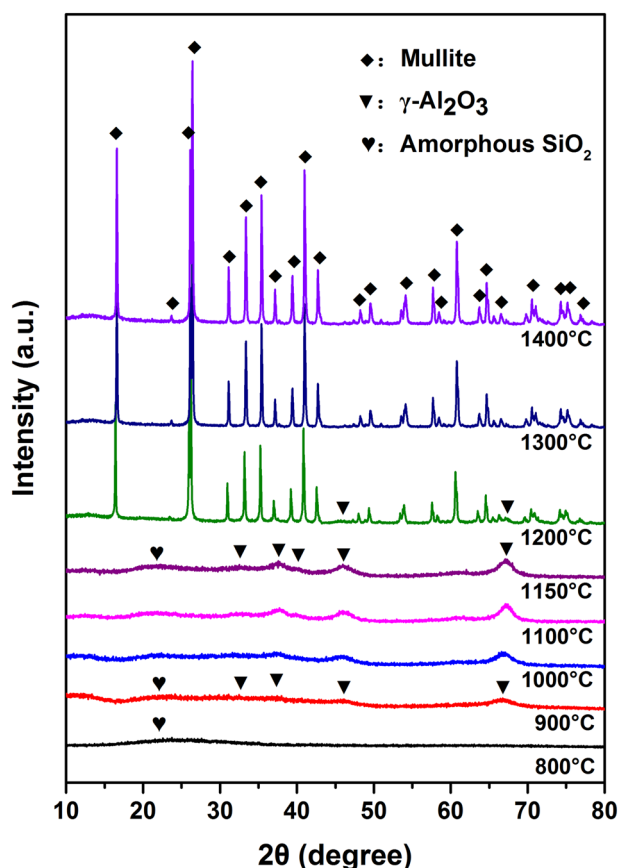


Fig. 6 XRD patterns of the diphasic mullite fibers sintered at different temperatures

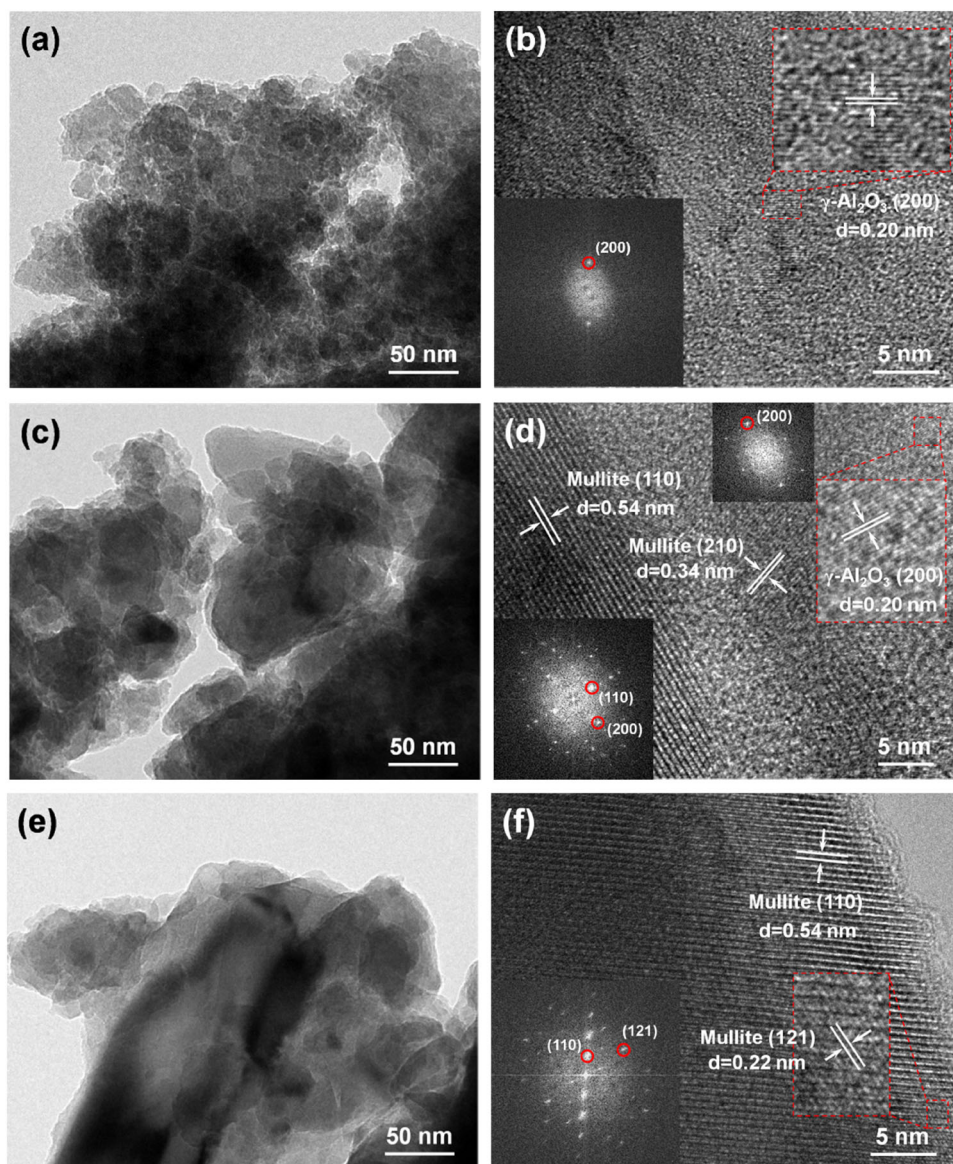
displayed the uniformly distributed Al, Si and O, revealing that the prepared fibers were chemically homogeneous. The EDS spectrum exhibited in Fig. 4d verified that the atomic percentage of Al and Si was 41.51 and 10.30%, respectively, which were basically equal to the designed values (41.43% for Al and 10.15% for Si). Besides, no carbon was not found in the sample, demonstrating the complete decomposition of organics after the pyrolysis process.

### 3.3 Microstructure and mechanical properties at elevated temperatures

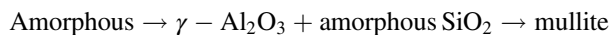
Figure 5 presents the DTA curve for the precursor fibers in the temperature range of 900 to 1400 °C. Two exothermic peaks were observed. The first peak located at 981 °C was assigned to the formation of  $\gamma$ -Al<sub>2</sub>O<sub>3</sub> phase and the second one at 1271 °C was due to the transformation to the mullite phase. These transformation temperatures coincided with the temperatures of onset of  $\gamma$ -Al<sub>2</sub>O<sub>3</sub> and mullite phase for diphasic mullite products [9]. The XRD patterns of the sintered fibers for phase identification are displayed in Fig. 6. At 800 °C, the broad peaks revealed that the sintered fibers were in the amorphous state, which was in consistent with the DTA result. At temperatures ranged from 900 to



**Fig. 7** TEM and HRTEM images of the diphasic mullite fibers sintered at **a, b** 1000 °C, **c, d** 1200 °C and **e, f** 1400 °C



1150 °C,  $\gamma$ - $\text{Al}_2\text{O}_3$  became the principal crystal phase and amorphous  $\text{SiO}_2$  was also identified. As the sintering treatments progressed, the diffraction peaks corresponded to mullite phase appeared and  $\gamma$ - $\text{Al}_2\text{O}_3$  almost disappeared at 1200 °C. In the range of 1300–1400 °C, mullite was the only phase presented in the fibers. From the above results, the phase evolution of diphasic mullite fibers in the current study could be summarized as follows:



This was the typical phase transformation route of diphasic mullite gel to mullite products during the sintering process. Besides, with the temperatures increased, the intensities of diffraction peaks for both  $\gamma$ - $\text{Al}_2\text{O}_3$  phase and mullite phase became increasingly strong, indicating that the crystallinities of the fibers improved.

Figure 7 shows the TEM and HRTEM images of the diphasic mullite fibers sintered at different temperatures for 0.5 h. From Fig. 7a, c, e it could be found that the crystal grain sizes increased significantly at higher temperatures. When sintered at 1000 °C, as displayed in Fig. 7b, the formed  $\gamma$ - $\text{Al}_2\text{O}_3$  grains with sizes smaller than 15 nm were surrounded by amorphous silica and showed crystallographic orientation in (200) crystal plane. At 1200 °C, Fig. 7d manifested that the fibers were composed of mullite grains,  $\gamma$ - $\text{Al}_2\text{O}_3$  grains and amorphous  $\text{SiO}_2$ . Thereinto, the mullite grains with sizes ranged from 10 to 50 nm mainly grew up in the directions of (110) and (210) crystal faces and the inlaid tiny  $\gamma$ - $\text{Al}_2\text{O}_3$  grains still showed the crystallographic orientation in (200) crystal plane. After sintering at 1400 °C, the sizes of mullite grains were larger than 200 nm. Figure 7f revealed that the grains grew up in the directions of (110) and (121) crystal faces.

**Fig. 8** Surface morphology of the diphasic mullite fibers sintered at different temperatures: **a** 900 °C, **b** 1000 °C, **c** 1100 °C, **d** 1200 °C, **e** 1300 °C and **f** 1400 °C

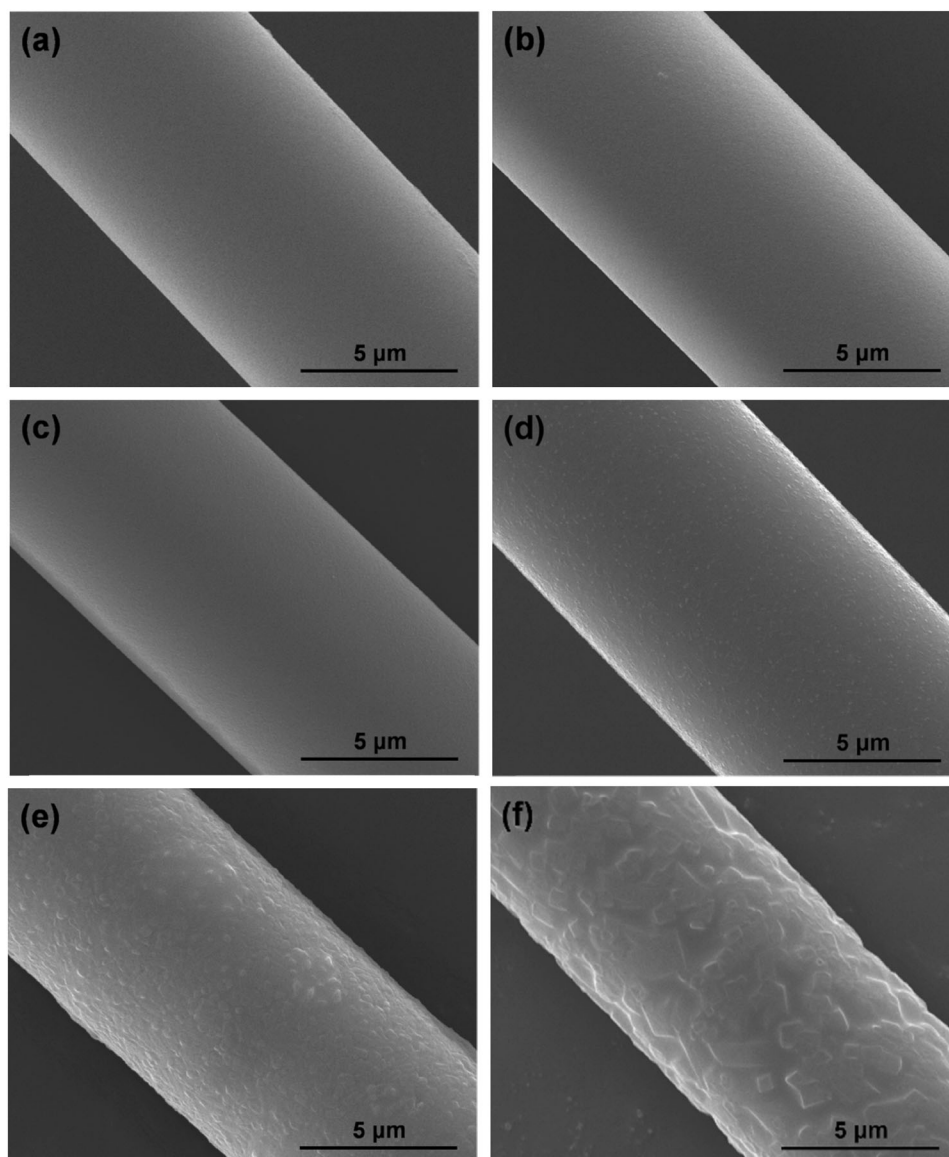
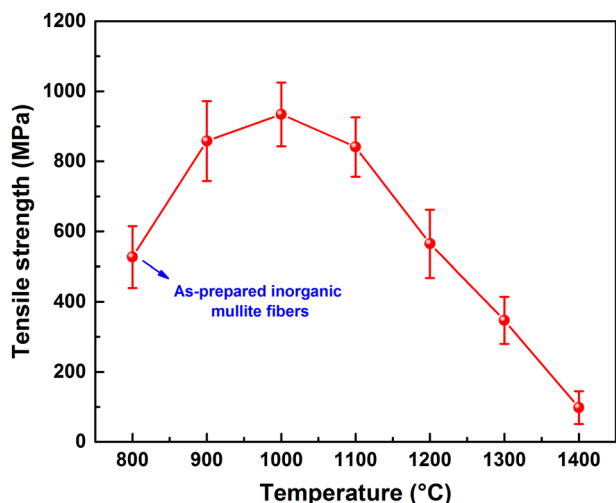


Figure 8 presents the surface morphology of the diphasic mullite fibers sintered at different temperatures. It could be found that the fibers sintered from 900 to 1100 °C had dense and smooth surface. Such a phenomenon was in accordance with the results as reported by previous literature [14, 25]. In this temperature range, XRD and TEM results showed that the fibers were composed of  $\gamma$ - $\text{Al}_2\text{O}_3$  grains and amorphous  $\text{SiO}_2$  and the  $\gamma$ - $\text{Al}_2\text{O}_3$  grains were surrounded by amorphous  $\text{SiO}_2$  phase, thereby leading to a slow grain growth rate upon sintering at higher temperatures. Therefore, the morphological characteristics did not change drastically. At 1200 °C, tiny particles resulted from the phase transformation and rapid grain growth emerged on the fiber surface. As temperature raised continuously to 1400 °C, it was apparent that the particles became irregular

and increasingly larger, which might straightly lead to the strength degradation of the fibers.

The filament tensile strength of the diphasic mullite fibers sintered at different temperatures is shown in Fig. 9. As observed, the tensile strength of the as-prepared inorganic mullite fibers was 527 MPa. For the fibers in the amorphous state, atoms were less constrained and the bond energy was relatively weak, thereby leading to a low strength value. When the sintering temperature reached up to 1000 °C, the strength value increased to 934 MPa due to the well-proceeded densification process. A decreased tendency of the fiber tensile strength caused by the grain growth was found along with the increasing sintering temperatures. For the sample obtained at 1400 °C, the fiber tensile strength reduced to 98 MPa. The tensile strength of



**Fig. 9** Relationship between filament tensile strength and sintering temperatures of the diphasic mullite fibers

the mullite fibers in the current work was lower than that of the commercial fibers as reported in Dong's studies [6]. The tensile strength of the as-received mullite fibers was 1723 MPa and it decreased to 191 MPa after calcining at 1500 °C. One possibility for this was the fiber processing method. As well known, fiber processing of the sol-gel derived commercial ceramic fibers is normally accomplished by dry spinning technique. Some unique technologies, such as coating organic sizes on the precursor fibers, exerting tension on the amorphous fibers, *etc.* are adopted [12, 26]. They are beneficial to acquire fiber products with improved mechanical properties. Nevertheless, those useful technologies were unrealizable for the draw-spinning mullite fibers in this study. That was to say, strength improvement for our mullite fibers could be achieved after optimizing the fabricating method.

## 4 Conclusion

Continuous mullite fibers were successfully prepared through the diphasic sol-gel route due to the high mullite formation temperatures and excellent thermal stability. Precursor fibers with continuous structure, smooth surface and dense feature were obtained via draw-spinning method. Upon heating the precursor in air, an overall ceramic yield of 43.7% at 720 °C was measured. After pyrolyzing at 800 °C, amorphous mullite fibers with designed chemical composition and uniform elemental distribution were obtained. DTA results showed that  $\gamma$ -Al<sub>2</sub>O<sub>3</sub> and mullite phases formed at 978 and 1271 °C, respectively, which verified the diphasic feature of the fibers. For the sample sintered at 1200 °C, mullite phase emerged and  $\gamma$ -Al<sub>2</sub>O<sub>3</sub> almost disappeared. Before mullite formation, the growth

rate of  $\gamma$ -Al<sub>2</sub>O<sub>3</sub> grains was relatively slow due to the presence of amorphous silica, resulting in the smooth surface in the range of 900–1100 °C. Once the reaction between Al<sub>2</sub>O<sub>3</sub> and SiO<sub>2</sub> occurred, the grains grew rapidly, thereby leading to the increasingly rough surface at above 1200 °C. The tensile strength of the fibers increased first and decreased then with the increased sintering temperatures. At 1000 °C, a maximum value of 934 MPa was obtained. The as-prepared fibers are an ideal candidate as the reinforcements for ceramics, and have promising application in the field of thermal storage.

**Acknowledgements** We gratefully acknowledge the financial support from the “Chang Jiang Scholars Program” of the Ministry of Education of China (Grant no. T2011119).

## Compliance with ethical standards

**Conflict of interest** The authors declare that they have no conflict of interest.

**Publisher's note:** Springer Nature remains neutral with regard to jurisdictional claims in published maps and institutional affiliations.

## References

- Bunsell AR, Berger MH (2000) Fine diameter ceramic fibres. *J Eur Ceram Soc* 20:2249–2260
- Deléglise F, Berger MH, Jeulin D, Bunsell AR (2001) Microstructural stability and room temperature mechanical properties of the Nextel 720 fibre. *J Eur Ceram Soc* 21:569–580
- Schawaller D, Clauß B, Buchmeiser MR (2012) Ceramic filament fibers - a review. *Macromol Mater Eng* 297:502–522
- Almeida RSM, Bergmüller EL, Eggert BGF, Tushtev K, Schumacher T, Lührs H, Clauß B, Grathwohl G, Rezwani K (2016) Thermal exposure effects on the strength and microstructure of a novel mullite fiber. *J Am Ceram Soc* 99:1709–1716
- Schneider H (2005) Basic Properties of Mullite. In: Schneider H, Komarneni S (eds) *Mullite*. Wiley-VCH, Weinheim, p 141–215
- Dong X, Chen Z, Guo A, Liu J, Wang X, Chen C (2018) Mechanical and interfacial behavior of single mullite fiber and mullite fiber-based porous ceramics. *Ceram Int* 44:14446–14456
- Okada K, Yasohama S, Hayashi S, Yasumori A (1998) Sol-gel synthesis of mullite long fibres from water solvent systems. *J Eur Ceram Soc* 18:1879–1884
- Song KC (1998) Preparation of mullite fibers from aluminum isopropoxide-aluminum nitrate-tetraethylorthosilicate solutions by sol-gel method. *Mater Lett* 35:290–296
- Cividanes LS, Campos TMB, Rodrigues LA, Brunelli DD, Thim GP (2010) Review of mullite synthesis routes by sol-gel method. *J Sol-Gel Sci Technol* 55:111–125
- Chen X, Gu L (2009) Sol-gel dry spinning of mullite fibers from AN/TEOS/AIP system. *Mater Res Bull* 44:865–873
- Zhang Y, Ding Y, Gao J, Yang J (2009) Mullite fibres prepared by sol-gel method using polyvinyl butyral. *J Eur Ceram Soc* 29:1101–1107
- Sowman HG (1974) Aluminum borate and aluminum borosilicate articles. US Patent 3,795,524.
- Schmücker M, Flucht F, Schneider H (1996) High temperature behaviour of polycrystalline aluminosilicate fibres with mullite



- bulk composition. i. microstructure and strength properties. *J Eur Ceram Soc* 16:281–285
14. Wang Y, Cheng H, Liu H, Wang J (2013) Microstructure and room temperature mechanical properties of mullite fibers after heat-treatment at elevated temperatures. *Mater Sci Eng A* 578:287–293
  15. Wood TE, Wilson DM (1989) Microcrystalline alumina-based ceramic articles. US Patent 4,954,462.
  16. Richards EA, Goodbrake CJ, Sowman HG (1991) Reactions and microstructure development in mullite fibers. *J Am Ceram Soc* 74:2404–2409
  17. Song KC (1999) Preparation of mullite fibers by the sol-gel method. *J Sol-Gel Sci Technol* 13:1017–1021
  18. Chen X, Gu L (2009) Spinnability and structure characterization of mullite fibers via sol-gel-ceramic route. *J Non Cryst Solids* 355:2415–2421
  19. Liao S, Bai X, Song J, Zhang Q, Ren J, Zhao Y, Wu H (2017) Draw-spinning of kilometer-long and highly stretchable polymer submicrometer fibers. *Adv Sci* 4:1600480
  20. Leivo J, Lindén M, Rosenholm JM, Ritola M, Teixeira CV, Levänen E, Mäntylä TA (2008) Evolution of aluminosilicate structure and mullite crystallization from homogeneous nanoparticulate sol-gel precursor with organic additives. *J Eur Ceram Soc* 28:1749–1762
  21. Beran A, Voll D, Schneider H (2001) Dehydration and structural development of mullite precursors: An FTIR spectroscopic study. *J Eur Ceram Soc* 21:2479–2485
  22. Ksapabutr B, Gulari E, Wongkasemjit S (2004) Sol-gel transition study and pyrolysis of alumina-based gels prepared from alumatrane precursor. *Colloids. Surf A Physicochem Eng Asp* 233:145–153
  23. Jing C, Zhao X, Zhang Y (2007) Sol-gel fabrication of compact, crack-free alumina film. *Mater Res Bull* 42:600–608
  24. Dong X, Liu J, Li X, Zhang X, Xue Y, Liu J, Guo A (2017) Electrospun mullite nanofibers derived from diphasic mullite sol. *J Am Ceram Soc* 100:3425–3433.
  25. Jiang R, Liu H, Yang L, Sun X, Cheng H (2018) Mechanical properties of aluminosilicate fiber heat-treated from 800 °C to 1400 °C: Effects of phase transition, grain growth and defects. *Mater Charact* 138:120–126
  26. Borer A, Krogseng GP (1973) Method of firing dry spun refractory oxide fibers. US Patent 3,760,049.